

RADIOSCIENCE LABORATORY



STANFORD ELECTRONICS LABORATORIES
DEPARTMENT OF ELECTRICAL ENGINEERING
STANFORD UNIVERSITY · STANFORD, CA 94305

NONLINEAR LONGITUDINAL RESONANCE INTERACTION OF ENERGETIC CHARGED
PARTICLES AND VLF WAVES IN THE MAGNETOSPHERE

By

Slobodan Tkalcevic

May 1982

Technical Report E4-2311

Prepared Under

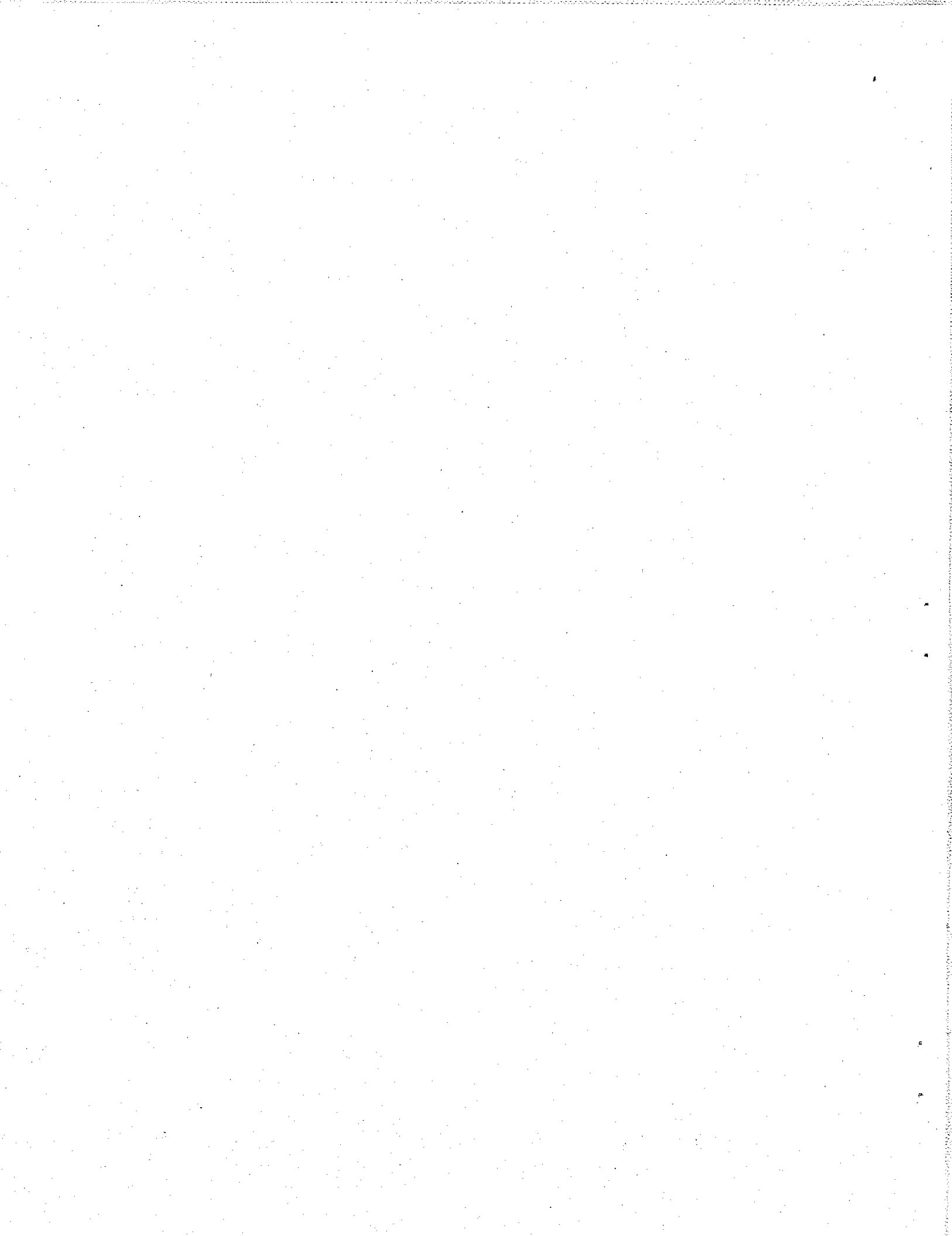
Division of Polar Programs of the National Science Foundation
Grants NSF-DPP80-22282 and DPP80-22540

Atmospheric Sciences Section of the National Science Foundation
Grant ATM80-18248

National Aeronautics and Space Administration
Grant NGL-05-020-008

ABSTRACT

This study treats the longitudinal resonance of waves and energetic electrons in the earth's magnetosphere, and the possible role this resonance may play in generating various magnetospheric phenomena. The first part of the study is concerned with the derivation of time-averaged nonlinear equations of motion for energetic particles longitudinally resonant with a whistler mode wave propagating with non-zero wave normal. It is shown that the wave magnetic forces can be neglected at lower particle pitch angles, while they become equal to or larger than the wave electric forces for $\alpha > 30^\circ$. The time-averaged equations of motion were used in test particle simulations which were done for a wide range of wave amplitudes, wave-normals, particle pitch angles, particle parallel velocities, and in an inhomogeneous medium such as the magnetosphere. It was found that there are two classes of particles, trapped and untrapped, and that the scattering and energy exchange for those two groups exhibit significantly different behavior. The trapped particles are characterized by a bounded phase variation (with respect to the wave) which is less than 2π , whereas the phase variation of untrapped particles is unbounded. It is also found that the trapping of the particles requires that the wave amplitude exceed a certain threshold value, and that the trapped electrons become space bunched due to the interaction. The full distribution simulations indicate that the expected particle precipitation is considerably smaller (one order of magnitude) compared to gyroresonance-induced precipitation for waves of comparable amplitude, which shows that the scattering efficiency of the longitudinal resonance is small. The amplitude threshold effect, together with the space bunching effect, was found to support one of the mechanisms suggested to explain whistler precursors.



ACKNOWLEDGMENTS

This research was supervised by Professors R. A. Helliwell and D. L. Carpenter. The author wishes to thank them for their guidance and support, and for many helpful discussions during the course of this work. I wish to express appreciation to Dr. C. G. Park who first interested me in problems of longitudinal resonance interaction.

I would also like to thank Drs. U. S. Inan and T. F. Bell for their cooperation and many valuable discussions. Thanks are also due to W. Terluin who drafted the figures, and to K. Dean and K. Feas who assisted with the typescript.

This research was supported in part by NASA under grant NGL-05-020-008, in part by the Division of Polar Programs of the National Science Foundation under grants DPP80-22282 and DPP80-22540, and in part by the Division of Atmospheric Sciences of NSF under grant ATM80-18248. Much of the computer modeling was done by remote job entry using the facilities of the National Center for Atmospheric Research which is sponsored by the National Science Foundation.

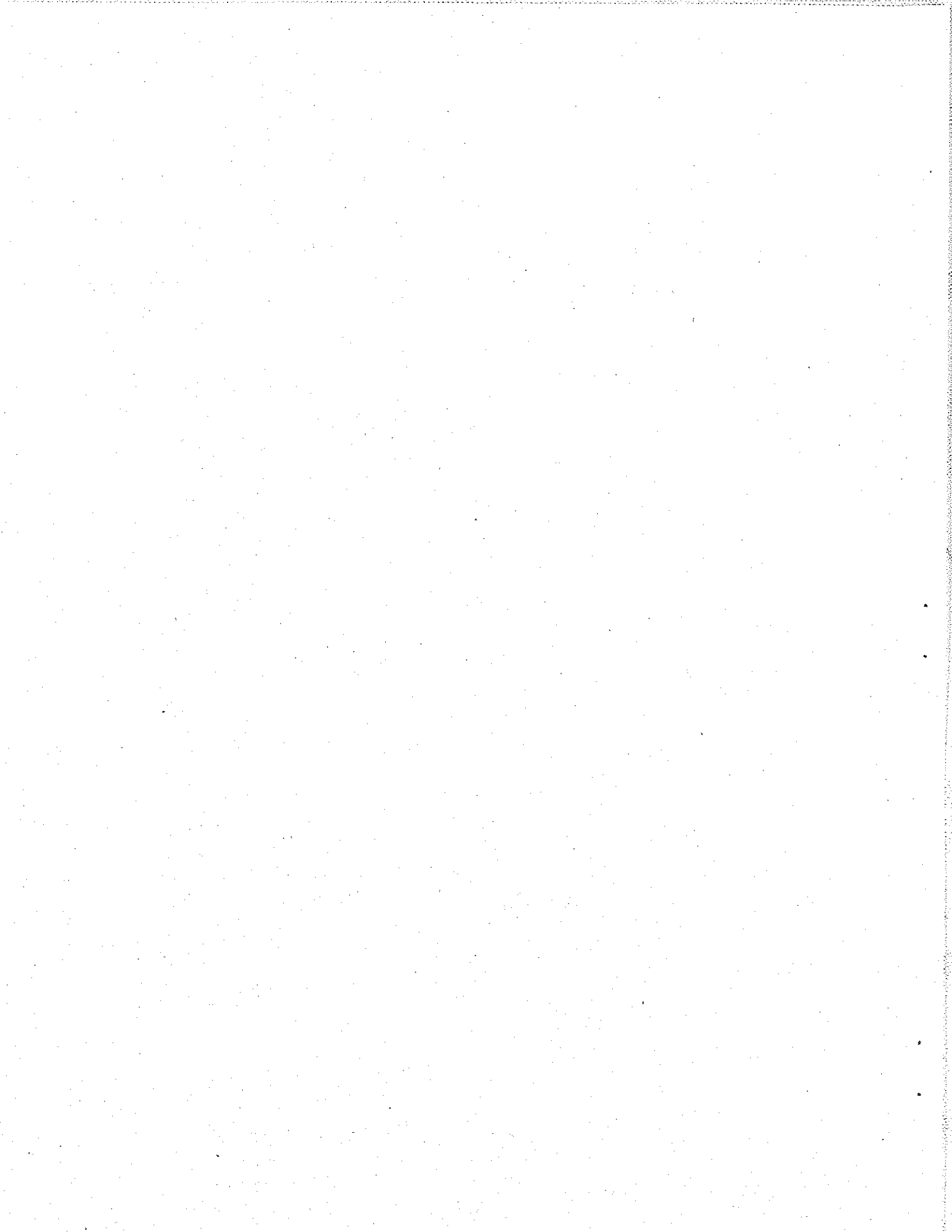


TABLE OF CONTENTS

Chapter	Page
I. INTRODUCTION	1
A. ORGANIZATION OF MATERIAL	1
B. WAVE-PARTICLE INTERACTIONS IN THE MAGNETOSPHERE	2
C. PREVIOUS WORK ON LONGITUDINAL RESONANCE	3
D. CONTRIBUTIONS OF THE PRESENT WORK	5
II. BASIC PHYSICS AND TIME AVERAGED EQUATIONS OF MOTION	8
A. MOTION OF PARTICLES IN EARTH'S MAGNETIC FIELD	8
B. LONGITUDINAL RESONANCE	11
C. NONLINEAR EQUATIONS OF MOTION FOR LANDAU INTERACTIONS WITH A WHISTLER MODE WAVE	18
D. TIME AVERAGING OF EQUATIONS OF MOTION	25
E. DISCUSSION OF FORCE EQUATIONS	29
III. ANALYTICAL STUDY OF LONGITUDINAL RESONANCE INTERACTION	37
A. INTRODUCTION	37
B. RELATION OF E_{\parallel} AND B_{\perp} AND MAGNITUDE OF E_{\parallel} FOR WHISTLER MODE SIGNALS	38
C. RESONANCE CONDITION $v_{\parallel} = v_{p\parallel}$	52
D. PHASE BETWEEN WAVE AND ELECTRON IN LONGITUDINAL RESONANCE	57
E. ENERGY EXCHANGE	63
IV. DESCRIPTION OF THE NUMERICAL SIMULATION	65
A. INTRODUCTION	65
B. COMPUTATION OF PROPAGATION AND ADIABATIC MOTION PARAMETERS	66
C. NUMERICAL INTEGRATION OF THE EQUATIONS OF MOTION	67
V. NUMERICAL ANALYSIS OF THE INTERACTION	74

TABLE OF CONTENTS (Cont.)

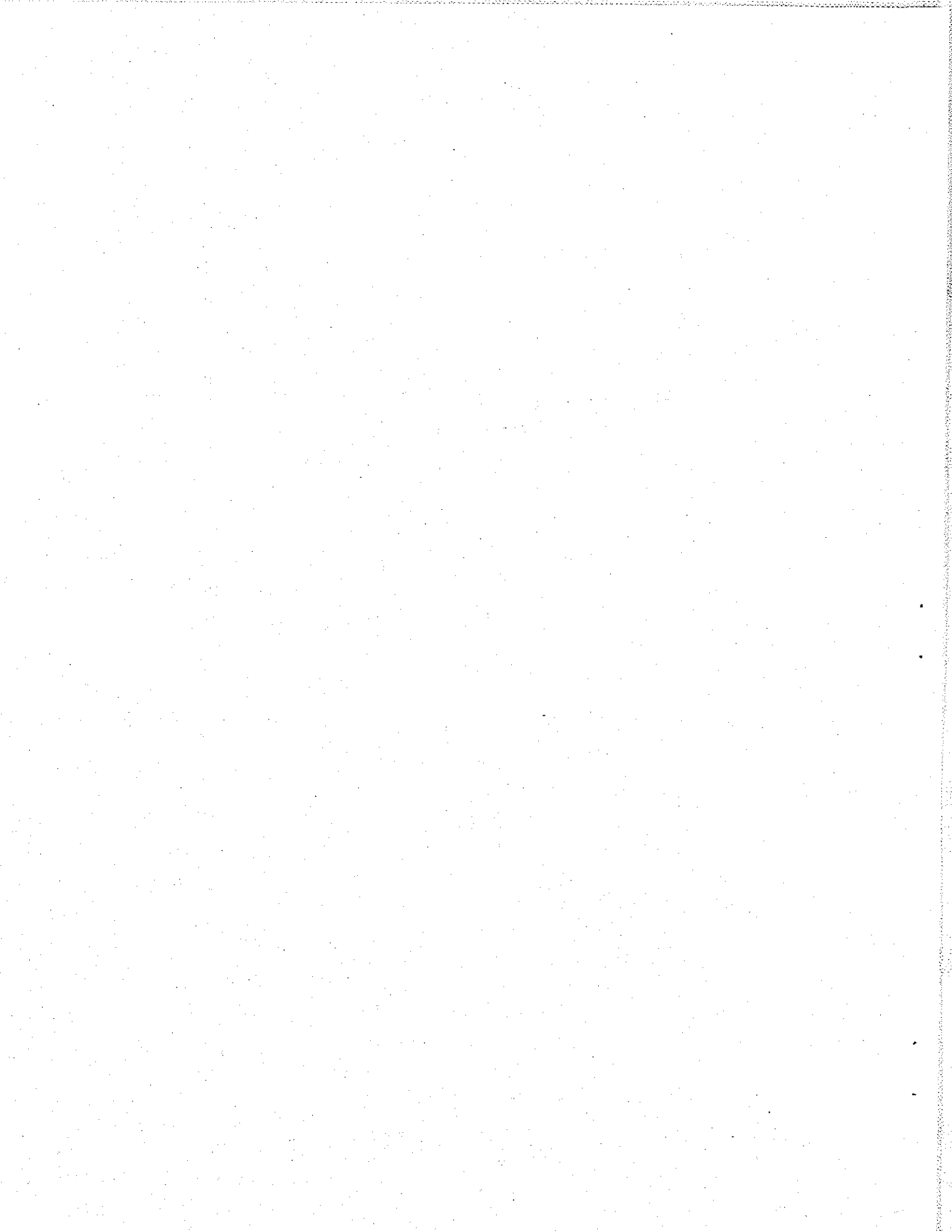
Chapter	Page
A. INTRODUCTION	74
B. SCATTERING OF A SINGLE SHEET INTERACTING WITH CW SIGNAL	75
C. SCATTERING OF A SINGLE SHEET INTERACTING WITH CW WAVES AMPLIFIED AT THE EQUATOR THROUGH THE CYCLOTRON RESONANCE	87
D. SCATTERING OF A SINGLE SHEET INTERACTING WITH SPATIAL PULSE	106
VI. FULL DISTRIBUTION SIMULATIONS	113
A. INTRODUCTION	113
B. PRECIPITATED ELECTRON FLUX	119
C. ENERGY EXCHANGE AND BALANCE	124
VII. APPLICATIONS TO MAGNETOSPHERIC PHENOMENA	131
A. GENERATION OF WHISTLER PRECURSORS	131
B. VLF HISS	147
C. COMMENTS ON THE INTERNAL FIELDS OF THE BUNCH	154
VIII. CONCLUSION AND SUGGESTIONS FOR FUTURE WORK	159
A. SUMMARY	159
B. SUGGESTIONS FOR FUTURE WORK	161
APPENDIX A.	164
APPENDIX B.	166
REFERENCES	188

LIST OF TABLES

Table	Page
3.1 Phase shift properties of longitudinally resonant electrons	62

LIST OF TABLES (Cont.)

Table		Page
5.1	Parameter values for the example case	75
7.1	Total number of electrons within 1% velocity band- width around $v_{ } = v_{p }$ as a function of flux and distribution function	157



ILLUSTRATIONS

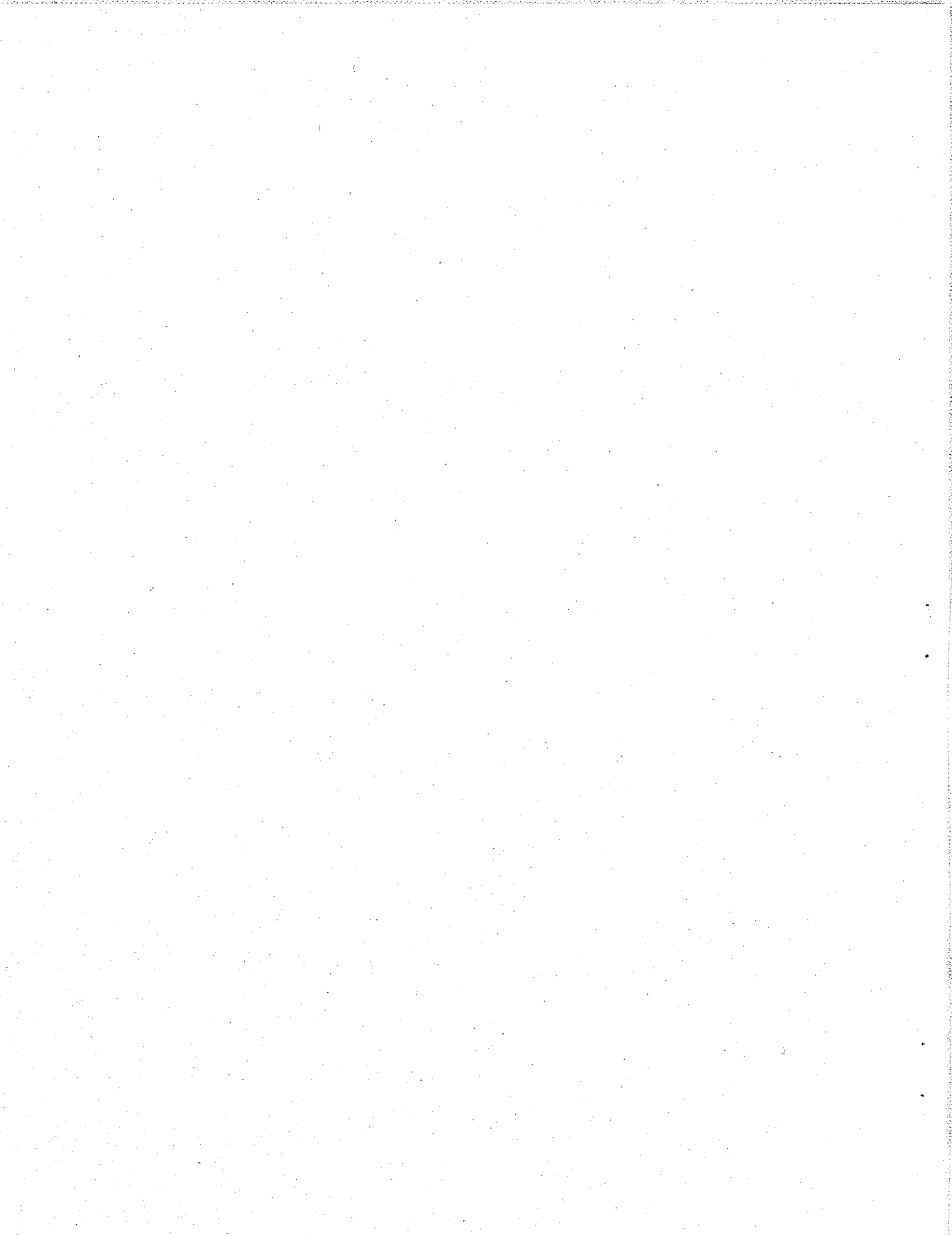
Figure		Page
2.1	Dipole geometry and symbols used for particle identification	9
2.2	Parallel electric field and the corresponding potential energy	15
2.3	Coordinate system for the equations of motion	19
2.4	Magnitude of the wave longitudinal polarization ρ_z as a function of wave normal angle	31
2.5	Normalized peak magnitudes of the $\langle qv_y \beta_x \rangle$ and $\langle q\mathcal{E}_z \rangle$ terms as functions of pitch angle	33
2.6	Normalized peak magnitudes of the $\langle qv_y \beta_x \rangle$ and $\langle q\mathcal{E}_z \rangle$ terms as functions of wave normal angle	34
2.7	Normalized peak magnitudes of the $\langle qv_y \beta_x \rangle$ and $\langle q\mathcal{E}_z \rangle$ terms as functions of normalized frequency f/f_H	35
3.1	Refractive index surface for $f < f_H/2$	42
3.2	Parallel electric field $E_{ }$ as a function of frequency for a whistler mode signal with $B_1 = 10$ pT	44
3.3	Parallel electric field $E_{ }$ as a function of frequency for a whistler mode signal, parametric in B_1	45
3.4	Parallel electric field $E_{ }$ as a function of frequency for a whistler mode wave propagating in the Gendrin mode	46
3.5	Parallel electric field $E_{ }$ as a function of wave normal angle θ	48
3.6	Normalized parallel electric field $E_{ }/B_1$ as a function of L value	49
3.7	Equatorial electron density as a function of L value	50
3.8	Equatorial parallel phase velocity as a function of L value	53
3.9	Parallel phase velocity as a function of latitude for different models of the distribution of electron density along the field line	54

ILLUSTRATIONS (Cont.)

Figure		Page
3.10	Normalized electron parallel velocity as a function of latitude	56
3.11	Relation between v_{\parallel} and $v_{p\parallel}$ along the field line . . .	58
4.1	Initial uniform phase distribution of electrons forming a test sheet	69
4.2	Interaction of the wave and a test particle	70
5.1	Mean scattering as a function of parallel velocity	77
5.2	Single electron trajectories for $B_{\perp} = 10$ pT	79
5.3	Single electron trajectories for $B_{\perp} = 10$ pT	81
5.4	Normalized energy of test sheet as a function of latitude	83
5.5	Single electron trajectories for $B_{\perp} = 10$ pT	86
5.6	Mean scattering as a function of parallel velocity	88
5.7	Mean scattering as a function of parallel velocity	92
5.8	Mean scattering as a function of wave amplitude for amplified CW signal	93
5.9	Single electron trajectories for $B_{\perp} = 10$ pT	94
5.10	Single electron trajectories for $B_{\perp} = 10$ pT	95
5.11	Single electron trajectories for $B_{\perp} = 30$ pT	97
5.12	Total scattering, $\Delta\alpha_{eq}$, versus initial phase for different wave amplitudes	99
5.13	Normalized energy of test sheet as a function of latitude	100
5.14	Mean scattering as a function of wave normal angle	101
5.15	Phase bunching due to the longitudinal resonance	104
5.16	Comparison between the effects of longitudinal resonance interactions inside and outside the plasmopause	105

ILLUSTRATIONS (Cont.)

Figure	Page
5.17 Interactions with spatial amplitude pulse extending between $\lambda = -10^\circ$ and $\lambda = -7^\circ$	108
5.18 Mean scattering for interactions with a spatial amplitude pulse extending between $\lambda = -10^\circ$ and $\lambda = -7^\circ$	109
5.19 Interactions with spatial amplitude pulse extending between $\lambda = 7^\circ$ and $\lambda = 10^\circ$	110
5.20 Mean scattering for interactions with a spatial amplitude pulse extending between $\lambda = 7^\circ$ and $\lambda = 10^\circ$	111
6.1 Simulation of the distribution function	116
6.2 Unperturbed and perturbed electron distribution	118
6.3 Normalized electron distributions $f(\alpha)$	121
6.4 Energy transfer from electrons to wave for the amplified CW signal as a function of particle parallel velocity	127
6.5 Particle detector resolution and detection of longitudinal resonance effects	129
7.1 Spectrograms of three whistler precursor events recorded at the Siple/Roberval conjugate stations	132
7.2 Expanded spectrogram of the precursor at 1400 UT from Figure 7.1	133
7.3 Schematic illustration of the whistler precursor generation mechanism	136
7.4 Amplitude of whistler components associated with the precursor activity of August 2, 1973	143
7.5 Estimated location of whistler duct exit point for the precursor events of August 2, 1973	145
7.6 Cerenkov radiation conditions in a nondispersive medium	149
7.7 Cerenkov radiation in a dispersive medium	150



I. INTRODUCTION

A. ORGANIZATION OF MATERIAL

This study treats longitudinal resonance interactions between energetic electrons and VLF waves in the earth's magnetosphere. The aim was to derive suitable analytical methods for test particle studies, and then to use those methods to investigate various aspects of the longitudinal resonance process.

The first part of the study is concerned with the derivation of equations of motion and their applications to the longitudinal resonance for a wide range of magnetospheric parameters. The second part gives the results of the numerical simulation of wave-particle interactions. The numerical simulations are done using a test particle approach to determine the perturbations of pitch angle for various wave functions. Also investigated are the perturbations of the full particle distribution and the energy exchange process.

In conclusion the longitudinal resonance interaction is compared to the cyclotron resonance interaction, and is related to phenomena observed in the magnetosphere.

B. WAVE-PARTICLE INTERACTIONS IN THE MAGNETOSPHERE

The magnetosphere, a magnetized region extending from about 1000 km altitude up to distance of roughly 100,000 km from the earth, is filled with both 'cold' and 'hot' plasma; the cold plasma consists of electrons and protons with energies in the 0.1-1 eV range, while the hot plasma consists of energetic particles with higher energies in the range from 100 eV to tens of MeV. The cold plasma together with the earth's static magnetic field determines the wave propagation properties of the magnetosphere. The hot plasma is a source of energetic particles which participate in the wave-particle interactions that result in radio wave emissions. As seen from both ground and satellite observations the magnetosphere supports numerous modes of wave propagation. It can be shown that the hot plasma, due to its very low density, does not affect the wave dispersion properties of the magnetosphere, i.e. the dispersion of waves can be explained assuming that only cold plasma is present.

It is known that very-low-frequency waves can propagate in the magnetosphere with phase velocities much smaller than the velocity of light, and that those waves, called whistler-mode waves, can undergo interactions with energetic particles both through longitudinal resonance and cyclotron (gyro) resonance. In longitudinal resonance the particle parallel velocity is matched to the wave phase velocity, whereas in the cyclotron resonance the doppler-shifted frequency of the wave (shifted due to the particle parallel velocity) matches the gyrofrequency of the energetic particle. Both types of interactions may induce perturbations of the energetic particle distribution through

pitch angle scattering, and may also result in different types of radio wave emissions, wave amplification (growth) and wave attenuation. The purpose of this study is to investigate the longitudinal resonance interactions of energetic particles with whistler mode signals propagating at an oblique angle to the static magnetic field. The approach taken is to use a test particle analysis and to study how the resonance process depends on various parameters. The particle trajectories are then used to estimate other effects such as wave growth/damping and particle trapping and precipitation. The trajectory calculations were done using a set of nonlinear equations of motion which are averaged over one gyroperiod [Inan and Tkalcevic, 1982].

C. PREVIOUS WORK ON LONGITUDINAL RESONANCE

The longitudinal resonance process has been invoked by many authors to explain various magnetospheric wave phenomena. One of the early works considered the traveling-wave-tube type of process as a generation mechanism for VLF emissions [Gallet and Helliwell, 1959], and this process was also considered for amplification of whistler mode signals [Brice, 1961]. The traveling-wave-tube mechanism was also considered by Dowden [1962] as a possible mechanism of hiss generation. Bell [1964] derived linearized solutions for the trajectories of longitudinally resonant particles, but these have not been extended to cover the nonlinear regime. The various emission-generation theories have been reviewed by Brice [1964], including both Cerenkov radiation and the traveling wave amplification hypothesis. The Cerenkov mechanism

is a process in which charged particles radiate electromagnetic waves as they travel through a medium. The necessary condition for the existence of this type of radiation, called a coherence condition, is easily found, and is the same as the condition required for the longitudinal interaction between the wave and the particle. Therefore, it is evident that those two processes, the longitudinal resonance interactions and Cerenkov radiation, are based on the same physical principle.

The Cerenkov radiation mechanism has been suggested by many authors [Ellis, 1959, 1960; Dowden, 1960; McKenzie, 1963] in order to explain VLF hiss. The problem of stability of whistler mode signals, i.e. the possibility of wave growth, accounting both for longitudinal and gyroresonance effects, was discussed by Kennel and Petschek [1966], Kennel and Thorne [1967], and also by Brinca [1972]. The work on radiation from moving charged particles, which includes Cerenkov radiation, includes the analysis done by Liemohn [1965], Mansfield [1967], and Seshadri [1967]. A good review of work done on Cerenkov radiation, along with additional analysis of the hiss power density spectrum, was given by Taylor and Shawhan [1974]. Their work gives examples of the power spectral density of hiss, both measured [Gurnett, 1966; Gurnett and Frank, 1972], and calculated [Jorgensen, 1968; Lim and Laaspere, 1972]. Swift and Kan [1975] showed that an electron beam can excite a whistler mode instability near the resonance cone through the longitudinal resonance interaction. Maggs [1976] and Kumagai et al. [1980] investigated beam amplification due to Cerenkov radiation from longitudinally resonant electrons, and considered this type of beam instability as a generating mechanism of VLF hiss. The whistler

precursor generation mechanism of Park and Helliwell [1977] was based on modifications of the particle distribution function achieved through longitudinal interaction between whistlers and energetic electrons.

Most of the above studies were primarily concerned with wave growth calculations using the wave dispersion relation. On the other hand, the detailed nonlinear motion of longitudinally resonant particles was studied only for the case of electrostatic waves [Nunn, 1971; 1973]. Palmadesso [1973] derived equations of motion for a case of oblique propagation, and used particle trajectories to estimate the nonlinear time dependent Landau damping rate of the wave.

D. CONTRIBUTIONS OF THE PRESENT WORK

The motion of electrons longitudinally resonant with a whistler mode wave propagating at an angle to the static magnetic field is represented by a simple set of equations motion which are averaged over the cyclotron period. It is shown that these nonlinear equations are a very accurate representation of the electron motion for a wide range of magnetospheric parameters.

Using the time-averaged nonlinear equations of motion in numerical simulations involving whistler mode signals propagating in an inhomogeneous medium it was found that the effects of wave magnetic forces can be neglected for low pitch angles, high wave normal angle, and/or high normalized wave frequency. At the higher pitch angles the wave magnetic forces become very important and it is necessary to

include the additional force terms as derived.

The sample calculations indicate that there are two classes of electrons, distinguished by the behavior of their phases with respect to the wave. In a case when the phase variation is bounded, i.e. less than 2π , the electron is said to be trapped, whereas unbounded phase variation characterizes the untrapped electrons. The scattering and corresponding energy exchange for the trapped and untrapped electrons exhibit significantly different characteristics.

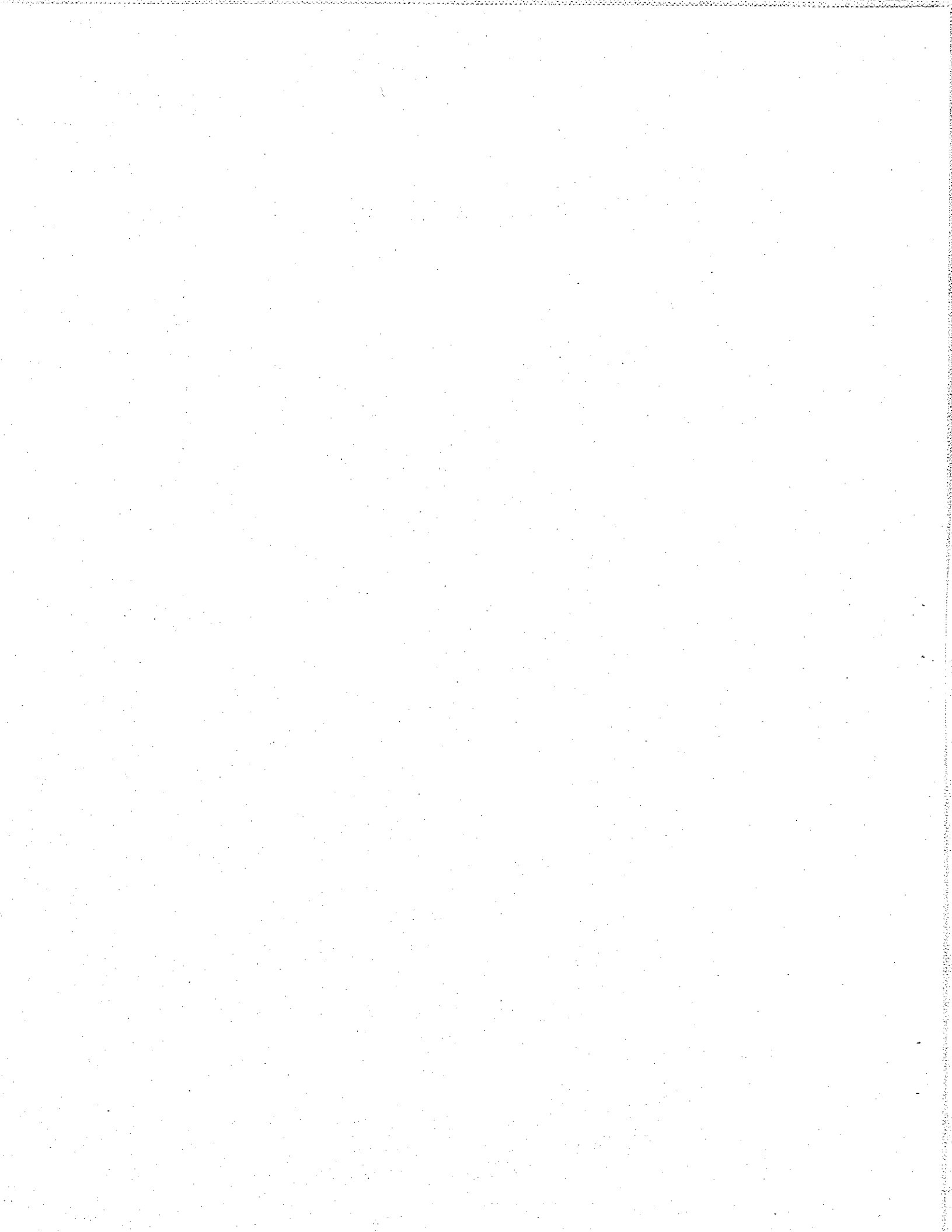
It is also found that the trapping of electrons is easier under conditions of spatial amplitude variation of a narrowband signal rather than for a constant amplitude. Analysis was done for a constant amplitude CW signal, a CW signal amplified at the equator through gyroresonance, and also for a spatial amplitude variation of the pulse formed by a nonducted signal.

It is also shown that the longitudinal resonance process involves a wave amplitude threshold effect, i.e. the trapping of electrons is possible only if the amplitude of the wave parallel electric field E_{\parallel} exceeds a certain value. The trapped electrons also become space bunched and temporarily increase the electron density over a particular range of parallel velocities.

The full distribution results show that the expected precipitation is small when compared to gyroresonance-induced precipitation for waves of comparable amplitude. In general, the results indicate that the longitudinal resonance scattering efficiency (scattering vs. amplitude) is considerably smaller, i.e. the efficiencies of the two processes differ by as much as an order of

magnitude.

The amplitude threshold effect was tested on whistler precursors, and it was found that the whistler amplitudes are well correlated with the occurrence of precursors, i.e. only whistlers with amplitudes above a certain threshold resulted in precursors. This provides support for the whistler precursor generation mechanism suggested by Park and Helliwell [1977], which involves longitudinal resonance interactions, and therefore it should exhibit a threshold effect as indicated by the measurements.



II. BASIC PHYSICS AND TIME AVERAGED EQUATIONS OF MOTION

A. MOTION OF CHARGED PARTICLES IN EARTH'S MAGNETIC FIELD

Motion of the charged energetic particles in the magnetosphere is governed by the earth's magnetic field. The earth's field in the inner magnetosphere can be approximated by the dipole model with the magnetic field strength B_0 given as

$$B_0 = 0.312 \cdot 10^{-4} (R_0/R)^3 \cdot (1 + 3\sin^2\lambda)^{1/2} \text{ Wb/m}^2 \quad (2.1)$$

where λ is the geomagnetic latitude, R is geocentric radius, and R_0 is the radius of the earth. The axis of the magnetic dipole is inclined with respect to the rotation axis by 11° .

The motion of a particle in the magnetosphere is uniquely described by either the parallel and perpendicular velocities of the particle, v_{\parallel} and v_{\perp} respectively, or by the parallel (perpendicular) velocity and pitch angle $\alpha = \arctan(v_{\perp} / v_{\parallel})$. Fig. 2.1 shows a typical geometry with the definitions of v_{\parallel} , v_{\perp} , and α .

It can be shown that for a spatially changing magnetic field, such as the earth's magnetic field given by Eq.2.1, charged particles will bounce forth and back along the field line between the mirror points [Northrop, 1963; Buneman 1980]. This is so because the particle perpendicular velocity must change in order to satisfy adiabatic

invariants, while the total kinetic energy of the particle must remain constant. The first adiabatic invariant is the invariance of the orbital magnetic moment, given as

$$W_{\perp}/B = \text{constant} \quad (2.2)$$

where W_{\perp} is the perpendicular kinetic energy of the particle.

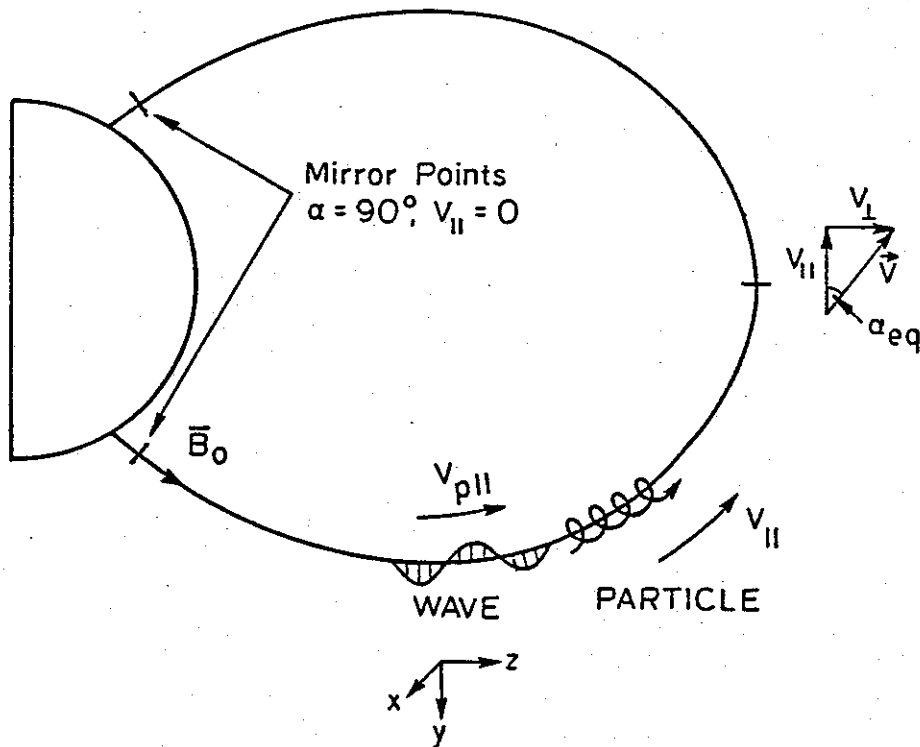


FIGURE 2.1 DIPOLE GEOMETRY AND SYMBOLS USED FOR PARTICLE IDENTIFICATION.

Note that the z -axis is aligned with the magnetic field line and that both the wave and the particles travel in the $+z$ direction. Particle orbits are described in terms of equatorial values of v_{\parallel} and α .

The second adiabatic invariant requires that the magnetic flux through the circle described by the particle gyrating around the field line remains constant, or

$$r_H^2 \times B = \text{constant} \quad (2.3)$$

where r_H is the electron gyroradius.

Thus if the magnetic field \bar{B}_0 increases, the perpendicular kinetic energy W_\perp must also increase according to Eq. 2.2. Furthermore, the parallel energy W_\parallel of the particle must decrease so that the total energy $W_\parallel + W_\perp$ remains constant. Therefore, the particle pitch angle $\alpha = \arctan\left(\sqrt{\frac{W_\perp}{W_\parallel}}\right)$ increases as \bar{B} increases up to the point where $\alpha = 90^\circ$. At this point the parallel velocity of the particle has been reduced to zero, and the particle begins to travel in the opposite direction along the same field line. When the particle reaches the conjugate point where again $\alpha = 90^\circ$, the process repeats. Hence the particle bounces back and forth along the magnetic field line between the two mirror points where $v_\parallel = 0$.

Finally, the motion of a particle trapped along a field line can be described by the following equations

$$\frac{dv_\parallel}{dt} = - \frac{v_\perp^2}{2B_0} \cdot \frac{dB_0}{dz} \quad (2.4)$$

$$\frac{dv_\perp}{dt} = + \frac{v_\parallel v_\perp}{2B_0} \cdot \frac{dB_0}{dz} \quad (2.5)$$

which can be derived from the first adiabatic invariant and the law of

energy conservation.

B. LONGITUDINAL RESONANCE

The bounce motion of the particles can be affected by resonant interactions between waves and the particles. The resonance condition is satisfied whenever the doppler-shifted frequency of the wave seen by the particle is equal to an integral multiple of the particle gyrofrequency, i.e.

$$\omega - k_{\parallel} v_{\parallel} = m\omega_H \quad m = 0, \pm 1, \pm 2, \pm 3, \dots \quad (2.6)$$

where ω is the wave frequency, k_{\parallel} is the wave number in the direction of the static magnetic field, and ω_H is the particle gyrofrequency.

The resonance condition given by Eq. 2.6 can be further divided into three subgroups according to different values of the parameter m . For $m > 0$ we have the resonance condition for the m -th order gyroresonance; $m < 0$ is the resonance condition for the m -th order anomalous gyroresonance; $m = 0$ yields the resonance condition for the longitudinal or Landau resonance. The last condition is given as

$$\omega - k_{\parallel} v_{\parallel} = 0 \quad (2.7)$$

or

$$v_{p\parallel} = v_{\parallel} \quad (2.8)$$

where $v_{p\parallel}$ is the wave phase velocity measured in the direction of the static magnetic field.

Before discussing the longitudinal resonance we should note that this resonance ($m=0$) is fully separable from the gyroresonances ($m\neq 0$), since the longitudinal resonance is possible only when the wave and the particles travel in the same direction, while the gyroresonance condition is satisfied only if the wave and the particles travel in the opposite direction. This separability of the different resonances makes their analysis much simpler. It is still possible for the same particle to interact simultaneously in both resonances with two different waves that satisfy corresponding resonant conditions. In this report we shall limit ourselves to discussion of the longitudinal resonance, although a comparison with the gyroresonance mechanism is given later in the text.

The condition given in Eq. 2.8 is the necessary condition for the longitudinal resonance. However, in order for the particle and the wave to exchange energy through the particle trapping process, the parallel component of the wave electric field must have a non-zero value. Therefore, even if the particle parallel velocity matches the wave phase velocity there will be no energy exchange between the particle and the wave if $E_{\parallel} = 0$. The direction of the energy exchange (whether wave or particle gains energy) depends on the initial velocity of the particle v_{\parallel} . In the case when v_{\parallel} is initially less than the phase velocity $v_{p\parallel}$ the particle will gain energy; if the initial v_{\parallel} is larger than $v_{p\parallel}$ the particle will lose some of its energy. We shall now present a simple analytical model for the longitudinal resonance and trapping process similar to that given by Seshadri [1973].

Let us assume that the longitudinal component of the wave electric field, propagating in the homogeneous medium, is given by

$$E_{\parallel}(s,t) = E_{\parallel 0} \sin(k_{\parallel} \cdot s - \omega \cdot t) \quad (2.9)$$

where s is the space coordinate. Eq. 2.9 is written in the laboratory coordinate system, but it is useful to do the analysis in the wave frame which moves at the phase velocity $v_{p\parallel}$. In this case a new space coordinate z is defined as

$$z = s - v_{p\parallel} t \quad (2.10)$$

Now, Eq. 2.9 can be rewritten as

$$E_{\parallel}(s,t) = E_{\parallel 0} \sin \left[k_{\parallel} \left(s - \frac{\omega}{k_{\parallel}} t \right) \right] \quad (2.11)$$

and using Eq. 2.10 and $v_{p\parallel} = \frac{\omega}{k_{\parallel}}$ Eq. 2.11 simplifies to

$$E_{\parallel}(z) = E_{\parallel 0} \sin(k_{\parallel} z) \quad (2.12)$$

The electric field given by the Eq. 2.12 is static in the wave frame and it is possible to derive a corresponding scalar potential $\Phi(z)$, by integrating $E_{\parallel}(\eta)$ where η is a dummy variable.

$$\Phi(z) = - \int_0^z E(\eta) \cdot d\eta \quad (2.13)$$

$$\phi(z) = - \int_0^z E_{\parallel 0} \sin(k_{\parallel} \eta) d\eta \quad (2.13a)$$

$$\phi(z) = \frac{E_{\parallel 0}}{k_{\parallel}} (\cos(k_{\parallel} z) - 1) \quad (2.13b)$$

Next we consider an electron (a similar derivation is possible for other types of charged particles) and its potential energy $W_p(z)$ which, in the wave frame is given by

$$W_p(z) = - e \cdot \phi(z) \quad (2.14)$$

$$W_p(z) = \frac{eE_{\parallel 0}}{k_{\parallel}} (1 - \cos(k_{\parallel} z)) = W_{p_{\max}} (1 - \cos(k_{\parallel} z)) \quad (2.14a)$$

The constant of the integration is chosen such that the minimum potential energy given by Eq. 2.14a is zero. Thus, the potential energy of the electron is a periodic function, as shown in Fig. 2.2.

It can be shown that the possibility of an electron being trapped depends on the initial kinetic energy of that electron measured in the wave frame. In a case when the initial kinetic energy of an electron, placed at z at the time $t=0$, is larger than the potential energy given by Eq. 2.14a, $W_{p_{\max}}$, there is no net interaction between the wave and electron, regardless of the electron initial velocity. The electron simply slides up and down the potential well as it moves either forward or backward through the wave, and there is no net energy exchange when averaged over one wavelength.

However, if the kinetic energy of the electron in the wave frame, $W_k(t=0)$, is less than the potential energy given by Eq. 2.14a,

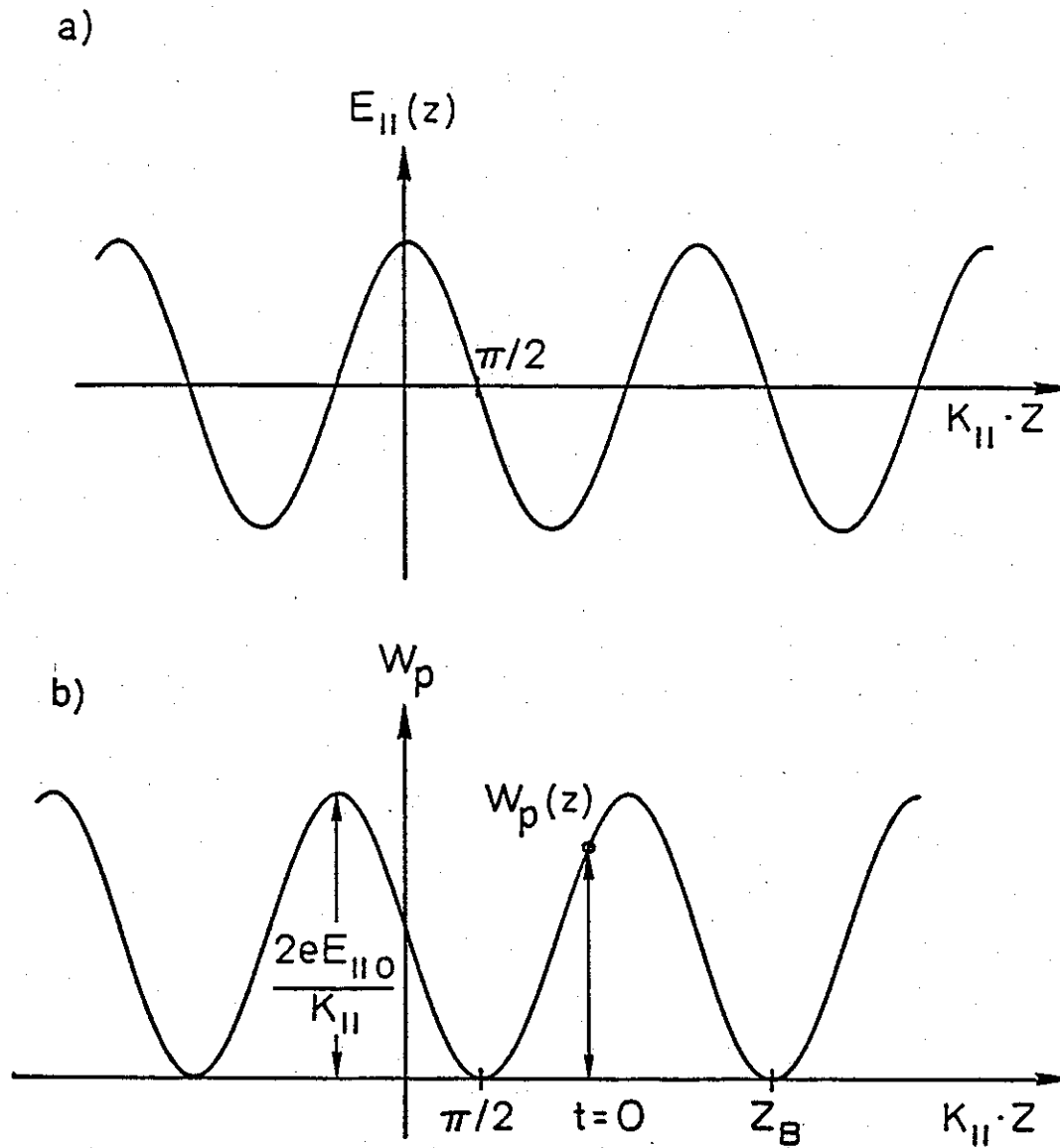


FIGURE 2.2 PARALLEL ELECTRIC FIELD AND THE CORRESPONDING POTENTIAL ENERGY. Both the parallel electric field $E_{||}$ and potential energy W_p of the electron are periodic functions in a reference frame moving at at the parallel phase velocity $v_{p||}$. In (b) z_B indicates the bottom of the potential well.

$W_{p_{\max}}$ as shown in Fig. 2.2 the electron is trapped in the potential well. The trapping condition is then given as

$$\frac{1}{2} m (v_{\parallel} - v_{p_{\parallel}})^2 < W_{p_{\max}} \quad (2.15)$$

$$\frac{1}{2} m (v_{\parallel} - v_{p_{\parallel}})^2 < \frac{eE_{\parallel 0}}{k_{\parallel}} \quad (2.15a)$$

$$|v_{\parallel} - v_{p_{\parallel}}| < \sqrt{\frac{2eE_{\parallel 0}}{mk_{\parallel}}} \quad (2.15b)$$

Rewriting the inequality of Eq. 2.15b as

$$v_{p_{\parallel}} - \sqrt{\frac{2eE_{\parallel 0}}{mk_{\parallel}}} < v_{\parallel} < v_{p_{\parallel}} + \sqrt{\frac{2eE_{\parallel 0}}{mk_{\parallel}}} \quad (2.16)$$

we have a range of velocities for which it is possible to trap an electron. Therefore, all electrons with parallel velocities that satisfy Eq. 2.16 are trapped in the wave potential well. The trapping velocity bandwidth v_t is given as

$$v_t = \sqrt{\frac{2eE_{\parallel 0}}{mk_{\parallel}}} \quad (2.17)$$

Furthermore, it can be shown that the total energy, ΔW , exchanged between the wave and electrons during the trapping process is

$$\Delta W = \int_{v_{p_{\parallel}} - v_t}^{v_{p_{\parallel}} + v_t} f(v_{\parallel}) \Delta E dv_{\parallel} \quad (2.18)$$

where $f(v_{\parallel})$ is the electron distribution function; ΔE is the amount of

energy exchanged through trapping of a single electron, and it is expressed as

$$\Delta E = \frac{1}{2} m (v_{p\parallel} + \hat{v}_{\parallel})^2 - \frac{1}{2} m v_{\parallel}^2 \quad (2.19)$$

$$\Delta E = - m_e v_{p\parallel} (v_{\parallel} - v_{p\parallel}) \quad (2.19a)$$

where \hat{v}_{\parallel} is a time-varying periodic function describing the oscillation of an electron at the bottom of the potential well. Expanding $f(v_{\parallel})$ in a Taylor series around $v_{\parallel} = v_{p\parallel}$ we obtain

$$f(v_{\parallel}) = f(v_{p\parallel}) + (v_{\parallel} - v_{p\parallel}) \left. \frac{\partial f(v_{\parallel})}{\partial v_{\parallel}} \right|_{v_{\parallel} = v_{p\parallel}} \quad (2.20)$$

and finally substituting Eq. 2.20 in Eq. 2.18 the total energy exchanged in the trapping process, ΔW , is given as

$$\Delta W = -\frac{2}{3} m v_{p\parallel} v_t^3 f'(v_{p\parallel}) \quad (2.21)$$

The result derived in Eq. 2.21 shows that the net energy exchanged between the trapped electrons and the wave depends on the slope of the distribution function at a point where the electron velocity is equal to the phase velocity of the wave. In the case when the number of electrons moving faster is larger than the number of electrons moving slower than the phase velocity, the wave gains energy and its amplitude grows. Similarly, if the number of slow electrons is larger than the number of fast electrons, the amplitude of the wave is

reduced.

The above analysis, using a longitudinal plasma wave and one-dimensional distribution function $f(v_{||})$, has demonstrated that it is possible to have wave damping in the absence of collisions, also known as Landau damping. It was also shown that the wave amplitude grows if the slope of the distribution function is positive. However, the expressions for the energy exchange were derived assuming that the particles are already trapped. It was also assumed that the medium is homogeneous, and that both the wave and the distribution function are one-dimensional.

In the magnetosphere Eq. 2.18 is still valid, but the trapping process is governed by the particle equations of motion. Thus in order to find the energy exchanged between a wave and particle (ΔE in Eq. 2.18) it is necessary to derive the equations of motion for a single particle when it is in longitudinal resonance with waves in the magnetosphere.

C. NONLINEAR EQUATIONS OF MOTION FOR LANDAU RESONANCE INTERACTIONS WITH A WHISTLER MODE WAVE

Now we consider an elliptically polarized wave propagating in the cold plasma of the magnetosphere with a static magnetic field \bar{B}_0 . The wave frequency f is assumed to be less than the electron gyrofrequency f_H ; in that case there is only one propagating wave [Ratcliffe, 1959; Budden, 1961], which is called a whistler wave.

In the most general case all Cartesian components of the wave electric \bar{E}_w and magnetic field \bar{B}_w have non-zero values. All of these components can be expressed in terms of \bar{E}_z through the cold-plasma dispersion relation. Without any loss of generality the wave vector \bar{k} is confined to the x - z plane, at an angle θ from the static magnetic field. The coordinate system used is shown in Fig. 2.3.

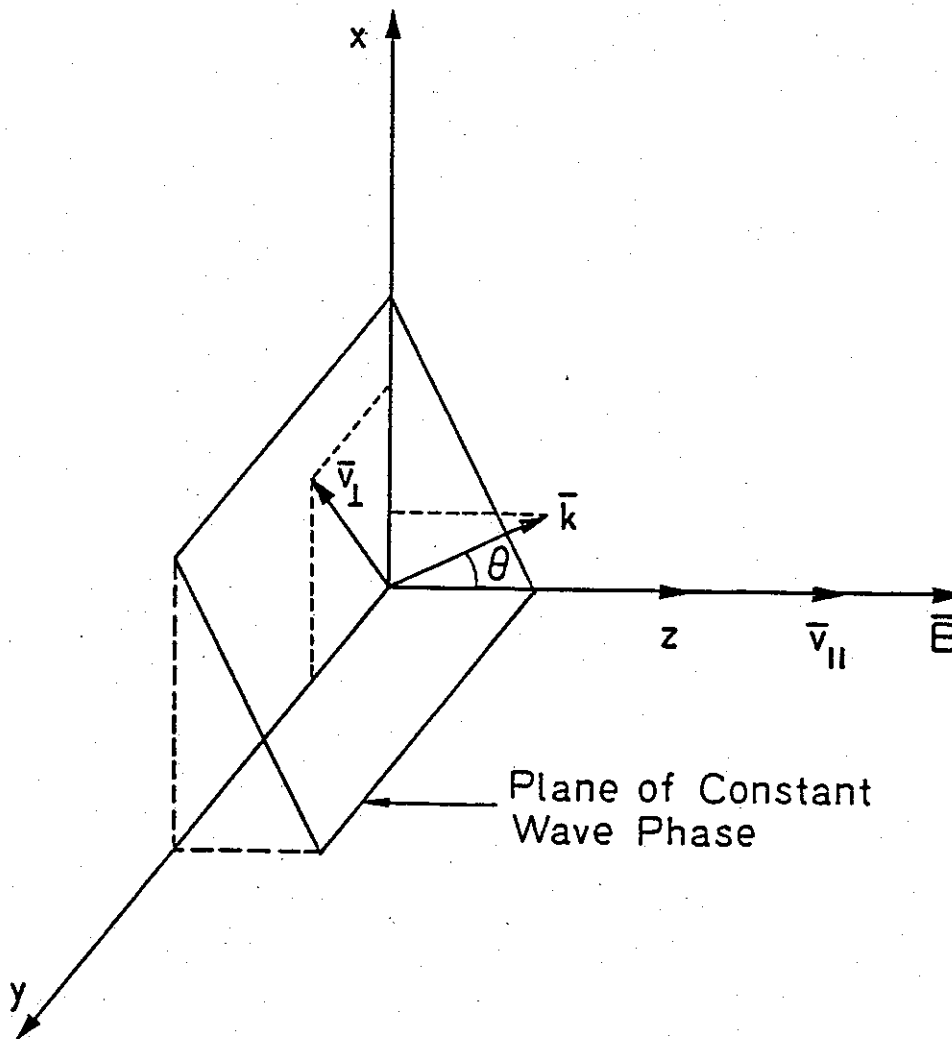


FIGURE 2.3 COORDINATE SYSTEM FOR THE EQUATIONS OF MOTION. The wave vector \bar{k} is at an angle θ from the static magnetic field \bar{B}_0 .

We also assume propagation as $\exp i(\omega t - \bar{k} \cdot \bar{r})$. Using a plasma dispersion relation [Stix, 1962]

$$\begin{vmatrix} \epsilon_1 - n^2 \cos^2 \theta & -i\epsilon_x & n^2 \sin \theta \cos \theta \\ i\epsilon_x & \epsilon_1 - n^2 & 0 \\ n^2 \sin \theta \cos \theta & 0 & \epsilon_{||} - n^2 \sin^2 \theta \end{vmatrix} \begin{vmatrix} \mathcal{E}_x \\ \mathcal{E}_y \\ \mathcal{E}_z \end{vmatrix} = 0 \quad (2.22)$$

all electric field components can be expressed in terms of \mathcal{E}_z as follows

$$\mathcal{E}_z = E_{||} \cos(\omega t - \bar{k} \cdot \bar{r}) \quad (2.23)$$

$$\mathcal{E}_x = \frac{n^2 \sin \theta - \epsilon_{||}}{n^2 \sin \theta \cos \theta} E_{||} \cos(\omega t - \bar{k} \cdot \bar{r}) \quad (2.24)$$

$$\mathcal{E}_y = \frac{\epsilon_x}{n^2 - \epsilon_1} \frac{n^2 \sin \theta - \epsilon_{||}}{n^2 \sin \theta \cos \theta} E_{||} \sin(\omega t - \bar{k} \cdot \bar{r}) \quad (2.25)$$

where $\epsilon_{||} = 1 - \frac{\omega_p^2}{\omega^2}$, $\epsilon_1 = 1 - \frac{\omega_p^2}{\omega^2 - \omega_H^2}$, $\epsilon_x = \frac{\omega_H}{\omega} \frac{\omega_p^2}{\omega^2 - \omega_H^2}$. The refractive index

n can be derived from Eq. 2.22 as (QL approximation)

$$n^2 = 1 + \frac{f_p^2}{f(f_H \cos \theta - f)} \quad (2.25a)$$

Using Maxwell's equation $\nabla \times \bar{E} = -\frac{\partial \bar{B}}{\partial t}$ the wave magnetic components are

$$\mathcal{B}_x = -\frac{k \cos \theta}{\omega} \mathcal{E}_y \quad (2.26)$$

$$B_y = \frac{k \cos \theta}{\omega} \xi_x - \frac{k \sin \theta}{\omega} \xi_z \quad (2.27)$$

$$B_z = \frac{k \sin \theta}{\omega} \xi_y \quad (2.28)$$

which can be also expressed in terms of ξ_z using Eqs. 2.23, 2.24, and 2.25.

The variation of the total electron velocity \bar{v} is governed by the Lorentz force equation

$$m \frac{d\bar{v}}{dt} = q [\bar{E}_w + \bar{v} \times (\bar{B}_w + \bar{B}_0)] \quad (2.29)$$

where m and q are electron mass and charge. For the case when $|\bar{B}_w| \ll |\bar{B}_0|$, the electron gyromotion can be assumed to be unaffected by the wave to the first order, so that the Cartesian components of the electron velocity vary as

$$v_z = v_{||} \quad (2.30)$$

$$v_x = v_{\perp} \cos(\omega_H t + \beta_0) \quad (2.31)$$

$$v_y = v_{\perp} \sin(\omega_H t + \beta_0) \quad (2.32)$$

where ω_H is the electron gyrofrequency and β_0 is the initial cyclotron phase. Furthermore, as long as the wave field is much smaller than the earth's magnetic field, it is permissible first to derive the force applied to an electron by the wave fields and then to superimpose the

adiabatic variation of v_{\perp} and v_{\parallel} . Therefore, the perturbation of the electron motion induced by the wave fields only is given by

$$m \frac{d\bar{v}}{dt} = q[\bar{E}_w + \bar{v} \times \bar{B}_w] \quad (2.33)$$

It is useful to examine each Cartesian component in Eq. 2.33 separately.

These three components are given as

$$F_x = q[\bar{E}_x + v_y \bar{B}_z - v_z \bar{B}_y] \quad (2.34)$$

$$F_y = q[\bar{E}_y + v_z \bar{B}_x - v_x \bar{B}_z] \quad (2.35)$$

$$F_z = q[\bar{E}_z + v_x \bar{B}_y - v_y \bar{B}_x] \quad (2.36)$$

Before investigating those equations we simplify $\cos(\omega t - \bar{k} \cdot \bar{r})$, which can be expressed as

$$\cos(\omega t - k \cos\theta \cdot z - k \sin\theta \cdot x) \quad (2.37)$$

or letting $\gamma = \omega t - k \cos\theta z$ in Eq. 2.37 we have

$$\cos(\gamma - k \sin\theta x) \quad (2.38)$$

Eq. 2.38 can be further simplified using the fact that

$$x = \frac{v_{\perp}}{\omega_H} \sin(\omega_H t + \beta_0) \quad (2.39)$$

which is derived by integrating Eq. 2.31. Finally, replacing x in Eq. 2.38 by (2.39)

$$\cos(\omega t - \vec{k} \cdot \vec{r}) = \cos(\gamma - \eta \sin\phi) \quad (2.40)$$

where $\phi = \omega_H t + \beta$ and $\eta = \frac{v_{\perp} k \sin\theta}{\omega_H}$.

Now, using the result derived in (2.40) we can rewrite three Cartesian components of the Lorentz force as

$$F_x = q [E_x \sin(\gamma - \eta \sin\phi) + v_{\perp} \sin\phi B_y \sin(\gamma - \eta \sin\phi) - v_{\parallel} B_z \cos(\gamma - \eta \sin\phi)] \quad (2.41)$$

$$F_y = q [E_y \sin(\gamma - \eta \sin\phi) + v_{\parallel} B_x \sin(\gamma - \eta \sin\phi) - v_{\perp} \cos\phi B_z \sin(\gamma - \eta \sin\phi)] \quad (2.42)$$

$$F_z = q [E_z \cos(\gamma - \eta \sin\phi) + v_{\perp} \cos\phi B_y \cos(\gamma - \eta \sin\phi) - v_{\perp} \sin\phi B_x \sin(\gamma - \eta \sin\phi)] \quad (2.43)$$

Note that E_x , E_y , E_z , B_x , B_y , and B_z are the real magnitudes of the fields, with the phase differences taken separately into account through $\frac{\sin}{\cos}(\gamma - \eta \sin\phi)$ terms.

At this point we have three equations which can be used to describe the motion of particles in resonance with a whistler wave. However, it is desirable to reduce the number of required equations to simplify numerical simulations. In this case it is useful to combine

the x and y components of the Lorentz force in one perpendicular component. This is done by taking the time derivative of the square of the perpendicular velocity $v_{\perp}^2 = v_x^2 + v_y^2$

$$v_{\perp}^2 = v_x^2 + v_y^2 \quad (2.44)$$

$$v_{\perp} \frac{dv_{\perp}}{dt} = v_x \frac{dv_x}{dt} + v_y \frac{dv_y}{dt} \quad (2.44a)$$

and multiplying it by m/v_{\perp}

$$m \frac{dv_{\perp}}{dt} = m \frac{v_x}{v_{\perp}} \frac{dv_x}{dt} + m \frac{v_y}{v_{\perp}} \frac{dv_y}{dt} \quad (2.45)$$

However, $\frac{v_x}{v_{\perp}} = \cos \phi$, $\frac{v_y}{v_{\perp}} = \sin \phi$, $m \frac{dv_{\perp}}{dt} = F_{\perp}$, $m \frac{dv_x}{dt} = F_x$, and $m \frac{dv_y}{dt} = F_y$, and (2.45) reduces to

$$F_{\perp} = \cos \phi F_x + \sin \phi F_y \quad (2.46)$$

Now, combining Eqs. 2.46, 2.41, and 2.42 the perpendicular force term is

$$\begin{aligned} F_{\perp} = & \cos \phi \{ q [E_x \sin(\gamma - \eta \sin \phi) + v_{\perp} \sin \phi B_y \sin(\gamma - \eta \sin \phi) \\ & - v_{\parallel} B_z \cos(\gamma - \eta \sin \phi)] \} \\ & + \sin \phi \{ q [E_y \sin(\gamma - \eta \sin \phi) + v_{\parallel} B_x \sin(\gamma - \eta \sin \phi) \\ & - v_{\perp} \cos \phi B_z \sin(\gamma - \eta \sin \phi)] \} \quad (2.47) \end{aligned}$$

The motion of a particle is now described in terms of the parallel and perpendicular forces, given respectively by Eqs. 2.43 and

2.47. If the $\frac{\sin}{\cos} (\gamma - \eta \sin \phi)$ terms in these equations are expanded (Appendix A), the result is an infinite series of harmonics at frequencies $n\omega_H$ with amplitudes given by $J_n(\eta)$. In a general formulation all terms must be kept and Eqs. 2.43 and 2.47 must be used as they stand. However, the equations can be considerably simplified when time averaged over one cyclotron period, T_H , because the higher order force terms ($n \geq 2$) vanish. Also, qualitatively, the $v_x \beta_y$ term should average out to zero since wave phase does not vary in the y-direction. In the next section we present the necessary conditions for the averaging to be valid, along with the time averaged equations of motion.

D. TIME AVERAGING OF EQUATIONS OF MOTION

Before averaging Eqs. 2.43 and 2.47 over one gyroperiod we have to make sure that the wave phase variations, as seen by the particles during one gyroperiod, are negligible. For the small field case this condition can be stated as

$$\omega - \bar{k \cdot \bar{v}} \ll \omega_H \quad (2.48)$$

which would certainly be the case for the Landau resonance described by

$$\omega - \bar{k \cdot \bar{v}} \approx 0 \quad (2.49)$$

Note that Eq. 2.49 is the equivalent of Eq. 2.8.

We have stated condition (2.48) assuming small amplitude waves. This requires that the wave field be small enough that it cannot move the particle by a substantial fraction of a wavelength during a gyroperiod. This condition can be stated as

$$|a_p| \frac{1}{f_H^2} \ll \frac{c}{nf} \quad (2.50)$$

where a_p is the peak parallel acceleration, c is the speed of light, n is the refractive index, $f = \frac{\omega}{2\pi}$ is the wave frequency and $f_H = \frac{\omega_H}{2\pi}$ is the electron gyrofrequency. The peak value of the parallel acceleration a_p during a gyroperiod can be taken to be that for $\phi = \frac{3\pi}{2}$ and $\gamma - \eta \sin\phi = \frac{\pi}{2}$. From Eq. 2.43 we have

$$|a_p| = \left| \frac{q}{m} (E_z - v_y B_x) \right| \quad (2.51)$$

In a order to express E_z in terms of B_x , we have from Eq. 2.25

$$\xi_y = \rho_z \xi_z \quad (2.52)$$

where $\rho_z = i \frac{\epsilon_x}{n^2 - \epsilon} \frac{n^2 \sin\theta - \epsilon_{\parallel}}{n^2 \sin\theta \cos\theta} = \frac{\xi_y}{\xi_z}$. Substituting Eq. 2.52 in Eq. 2.26

$$B_x = - \frac{k \cos\theta}{\omega} \rho_z E_z \quad (2.53)$$

or

$$E_z = - \frac{B_x}{\rho_z} \frac{\omega}{k \cos \theta} \quad (2.54)$$

Furthermore, for the near resonant particles $\frac{\omega}{k \cos \theta} = v_{p\parallel} = v_{\parallel}$ and Eq. 2.54 yields

$$E_z = - \frac{B_x}{\rho_z} v_{\parallel} \quad (2.55)$$

Replacing the E_z in Eq. 2.51 with the above expression the peak acceleration $|a_p|$ is

$$|a_p| = \left| \frac{q}{m} \left(- \frac{B_x}{\rho_z} v_{\parallel} - v_{\perp} B_x \right) \right| \quad (2.56)$$

$$|a_p| = \frac{q}{m} B_x v_{\perp} \left(1 + \frac{1}{|\rho_z| \tan \alpha} \right) \quad (2.56a)$$

where $\tan \alpha = \frac{v_{\perp}}{v_{\parallel}}$.

The final step is to substitute (2.56a) in (2.50) in order to get the condition on wave intensity for which the averaging of equations (2.43) and (2.47) is valid;

$$B_x \ll B_u = \frac{mf_{\parallel}^2 c}{qv_{\perp} n f} \frac{|\rho_z| \tan \alpha}{1 + |\rho_z| \tan \alpha} \quad (2.57)$$

Thus B_u represents the upper limit on wave magnetic field intensity.

Note that B_x is equal to the total transverse B_w for circularly

polarized whistler waves. Assuming B_u to have a value much higher

(> 100 times) than the typical field intensities for whistler mode

waves in the magnetosphere [Burtis and Helliwell, 1975], as shown later

in the text, we shall now time average Eqs. 2.43 and 2.47 over one gyroperiod. In doing so we use the identities derived in Appendix A. The averaged equations of motion become

$$\left\langle m \frac{dv_z}{dt} \right\rangle = \left\langle q \tilde{E}_z \right\rangle - \left\langle q v_y B_x \right\rangle \quad (2.58)$$

$$\left\langle m \frac{dv_\perp}{dt} \right\rangle = \left\langle q \tilde{E}_y \right\rangle - \left\langle q v_z B_x \right\rangle \quad (2.59)$$

or

$$m \frac{dv_\parallel}{dt} = q E_z J_0(\eta) \left[1 - \frac{v_\perp \cos\theta}{\omega} \rho_z \frac{J_1(\eta)}{J_0(\eta)} \right] \sin(\omega t - k z \cos\theta) \quad (2.60)$$

$$m \frac{dv_\perp}{dt} = -q \rho_z E_z J_1(\eta) \left[1 - \frac{v_\parallel k \cos\theta}{\omega} \right] \sin(\omega t - k z \cos\theta) \quad (2.61)$$

Since the brackets on the left hand sides are dropped, $\frac{dv_\parallel}{dt}$ and $\frac{dv_\perp}{dt}$ should be understood to be the average rates of change of v_\parallel and v_\perp , respectively.

Finally, for an inhomogeneous medium with \bar{B}_0 variable as in the magnetosphere, the adiabatic variations of v_\parallel and v_\perp can be superposed on the wave-induced perturbations as long as the variation of \bar{B}_0 in one wavelength is negligible. Thus the complete averaged nonlinear equations of motion become

$$\frac{dv_\parallel}{dt} = \frac{q}{m} E_z J_0(\eta) \left[1 - \frac{v_\perp k \cos\theta}{\omega} \rho_z \frac{J_1(\eta)}{J_0(\eta)} \right] \sin(\omega t - k z \cos\theta) - \frac{v_\perp}{2B_0} \frac{dB_0}{dz} \quad (2.62)$$

$$\frac{dv_{\perp}}{dt} = - \frac{q}{m} \rho_z E_z J_1(\eta) \left[1 - \frac{v_{\parallel} k \cos \theta}{\omega} \right] \sin(\omega t - k z \cos \theta) + \frac{v_{\parallel} v_{\perp}}{2B_0} \frac{dB_0}{dz} \quad (2.63)$$

We shall discuss the relative importance of the different terms in Eqs. 2.62 and 2.63 in the next section.

E. DISCUSSION OF FORCE EQUATIONS

Two terms of the parallel force are:

$$\langle q \mathcal{E}_z \rangle = q E_z J_0(\eta) \sin \gamma \quad (2.64)$$

$$\langle q v_y \mathcal{B}_x \rangle = - q E_z J_1(\eta) \rho_z \tan \alpha \sin \gamma \quad (2.65)$$

Also note that using (2.49)

$$\eta = v_{\perp} \frac{k \sin \theta}{\omega_H} = \frac{\omega}{\omega_H} \tan \theta \frac{k \cos \theta}{\omega} v_{\perp} \quad (2.66)$$

$$\eta = \frac{\omega}{\omega_H} \tan \theta \tan \alpha \quad (2.66a)$$

for near-resonant particles.

The term in (2.64) proportional to $q E_z J_0(\eta)$ is similar to the $q E_z$ term that would be present in the case of electrostatic waves. The

$J_0(\eta)$ represents the fact that the E_z field seen by the particle at different points in its transverse orbit is changing since E_z has a transverse phase variation given by $k \times \sin \theta$. The term in (2.65) represents the effect of the $q \bar{v} \times \bar{B}$ force, and the fact that since the plane of rotation of the particle and the wave polarization ellipse are at an angle $(\frac{\pi}{2} - \theta)$, there is a net longitudinal acceleration even after averaging over one gyroperiod. For cases in which (2.64) is the dominant term, the equations of motion for interaction with whistler mode waves are much the same as those for electrostatic waves [Nunn 1971, 1973].

Before comparing the relative magnitudes of (2.64) and (2.65) for the range of the parameters in the magnetosphere it should be noted that $\frac{dv_{\perp}}{dt}$, given by Eq. 2.61, becomes very small for near-resonant particles with $v_{\parallel} = v_{p\parallel}$. In this case $1 - \frac{v_{\parallel} k \cos \theta}{\omega} = 1 - \frac{v_{\parallel}}{v_{p\parallel}} = 0$, and the perpendicular motion of the particles is primarily governed by the adiabatic term of Eq. 2.63. In the following figures we present the magnitudes of (2.64) and (2.65), as well as the longitudinal polarization ρ_z as a function of different parameters.

Figure 2.4 shows a plot of the longitudinal polarization ρ_z as a function of the wave normal angle θ , for different values of normalized frequency $\frac{\omega}{\omega_H}$. The results are computed by using the cold plasma dispersion relation [Stix, 1962]. The longitudinal polarization is $\rho_z = \frac{\delta y}{\delta z}$, as defined in (2.52). A plasma frequency $f_p = 180$ kHz, corresponding to 400 el/cc at the magnetic equator at $L = 4$, along with the equatorial gyrofrequency $f_H = 13.65$ kHz, were used in computing ρ_z . For $f_p \gg f_H$ the value of ρ_z is not strongly dependent on f_p . Note from

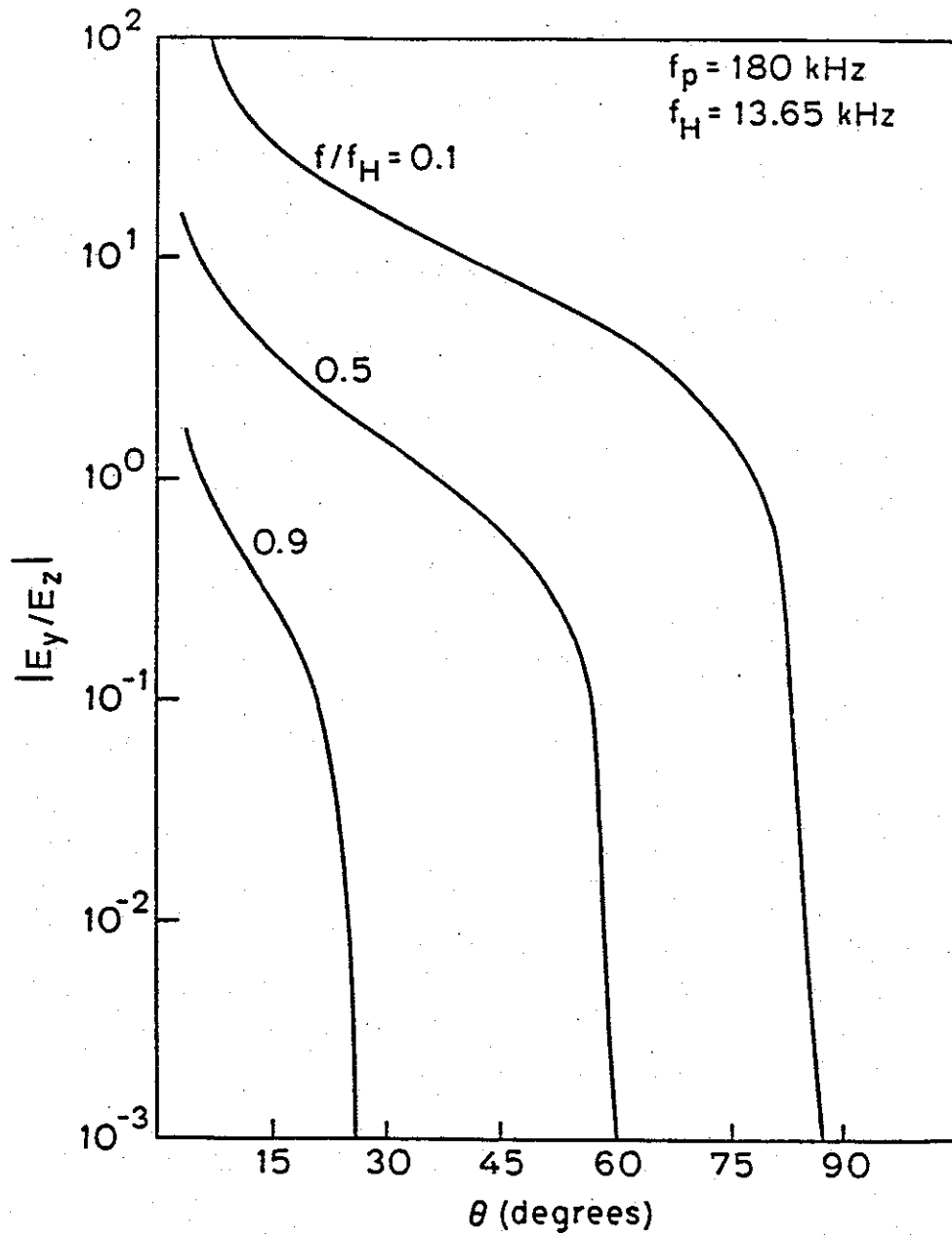


FIGURE 2.4. MAGNITUDE OF THE WAVE LONGITUDINAL POLARIZATION $|\rho_z| = |\epsilon_y/\epsilon_z|$ AS A FUNCTION OF WAVE NORMAL ANGLE θ . $|\rho_z|$ is shown for three different normalized frequencies.

Fig. 2.4 that ρ_z is in general higher at lower frequencies and decreases with increasing θ . Also recall that for longitudinal propagation, i.e., $\theta = 0^\circ$, $E_z = 0$ and there is no interaction between the particles and the waves.

Figures 2.5, 2.6 and 2.7 compare the peak magnitudes of the two terms as given by (2.64) and (2.65) for various parameters. Figure 2.5 shows variation of both terms with pitch angle α , for various wave normal angles θ and $f = 0.5 f_H$. It can be seen that the $\langle qv_y \mathcal{B}_x \rangle$ term is negligible for lower pitch angles, while it becomes equal to or larger than the $\langle q\mathcal{E}_z \rangle$ term for $\alpha > 30^\circ$. As long as $\alpha < 30^\circ$, the $\langle q\mathcal{E}_z \rangle$ term alone can be used to compute the motion of the Landau resonant particles with less than 10% error.

Figure 2.6 shows the dependence on the wave normal angle for various pitch angles α and for $f = 0.5 f_H$. The resonance cone angle for this frequency is $\approx 60^\circ$ as shown. This result indicates that for any pitch angle α , the $\langle qv_y \mathcal{B}_x \rangle$ term is more important at lower wave normal angles, but that there is a strong dependence on pitch angle as was also indicated in Figure 2.5. For θ approaching zero $J_1(\eta)$ goes to zero and ρ_z approaches infinity. As a result, the $\langle qv_y \mathcal{B}_x \rangle$ term will go to zero and may be approximated by $-qE_z \sin \eta \tan^2 \alpha (1 - f/f_H)/(2 + 2f/f_H)$ for small values of θ (Appendix A).

Finally, Figure 2.7 shows the variation of the terms with normalized frequency f/f_H . The curves are for $\alpha = 40^\circ$ and three different values of wave normal angle θ . It can be seen that the magnetic field term is more important at lower frequencies, although the dependence on frequency is not as strong as that on θ and α .

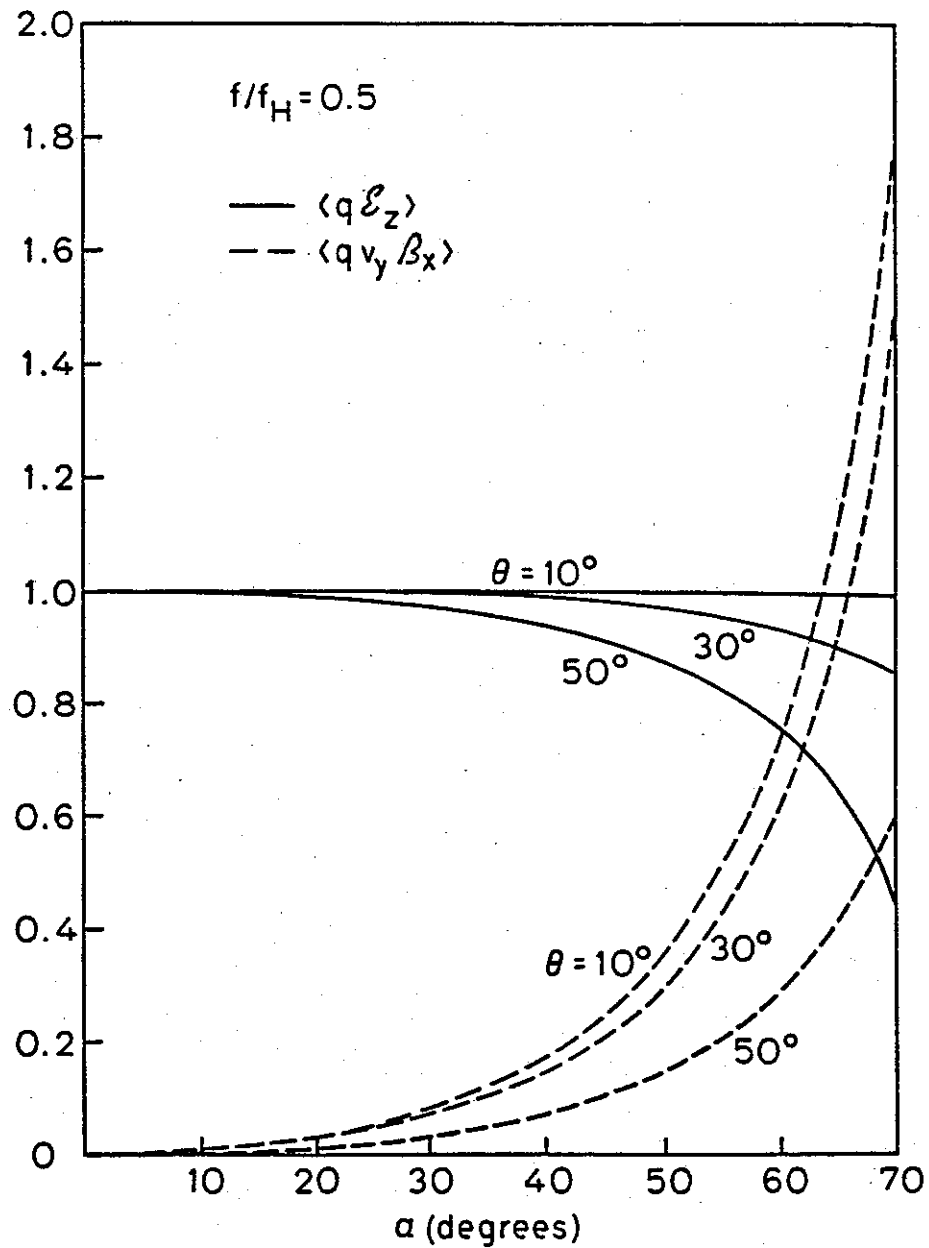


FIGURE 2.5 NORMALIZED PEAK MAGNITUDES OF THE $\langle q v_y \beta_x \rangle$ AND $\langle q \mathcal{E}_z \rangle$ TERMS AS FUNCTIONS OF PITCH ANGLE α . The results shown are for $f = 0.5 f_H$, and for three different wave normal angles θ .

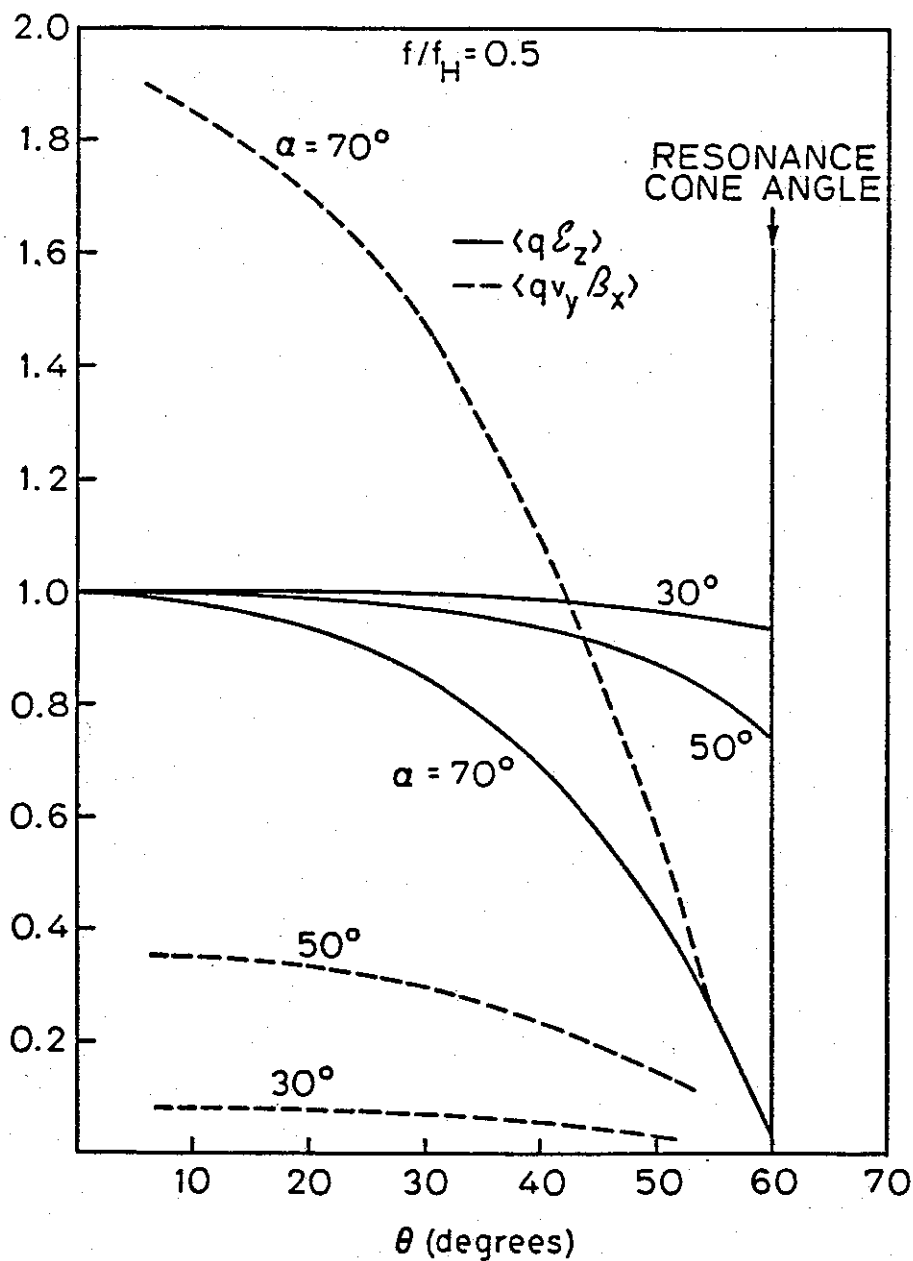


FIGURE 2.6 NORMALIZED PEAK MAGNITUDES OF THE $\langle qv_y \beta_x \rangle$ AND $\langle q\mathcal{E}_z \rangle$ TERMS AS FUNCTIONS OF WAVE NORMAL ANGLE θ . Both terms are calculated for three different pitch angles. The resonance cone angle for $f = 0.5 f_H$ is $\approx 60^\circ$ as shown.

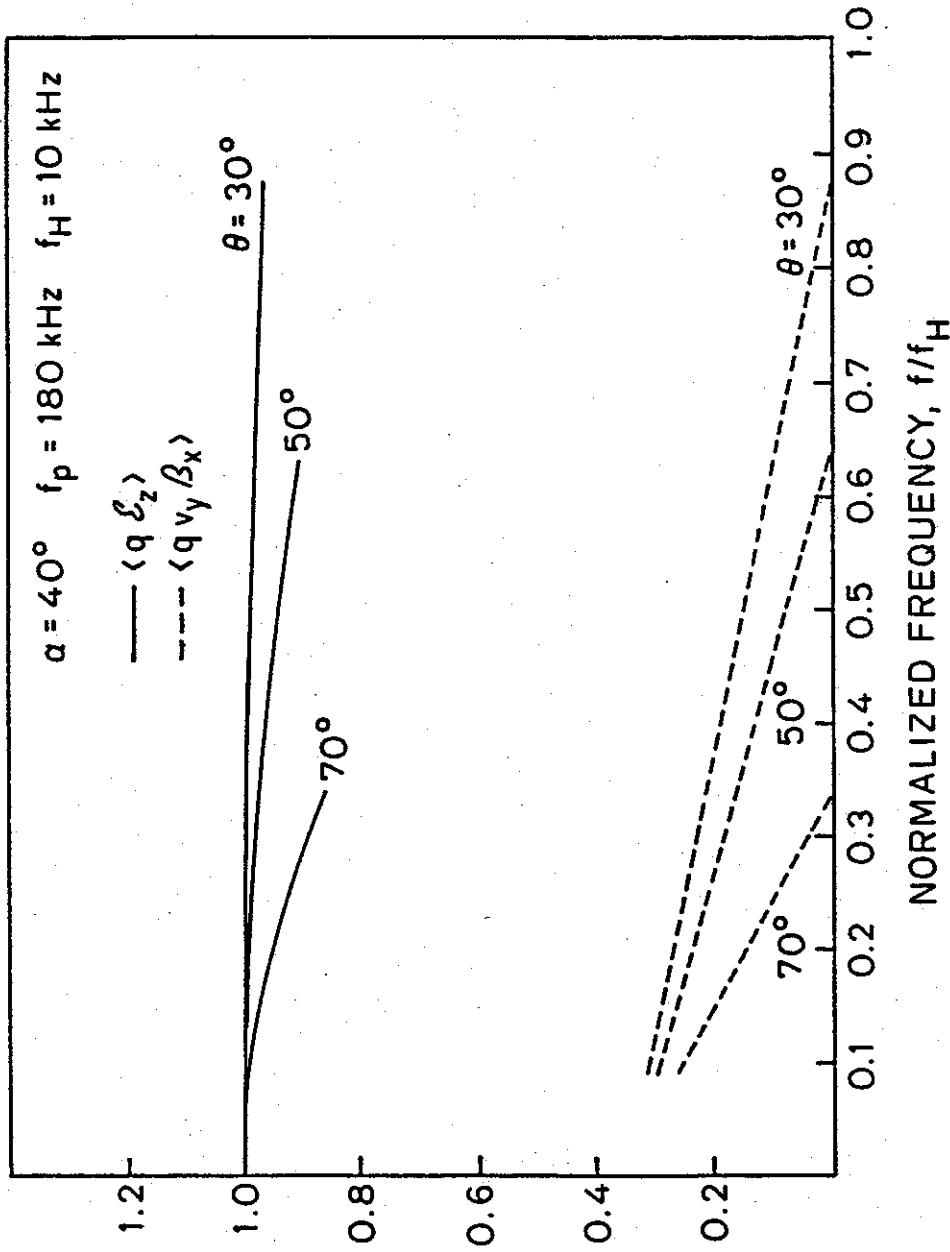


FIGURE 2.7 NORMALIZED PEAK MAGNITUDES OF THE $\langle q v_y \beta_x \rangle$ AND $\langle q \mathcal{E}_z \rangle$ TERMS AS FUNCTIONS OF NORMALIZED FREQUENCY f/f_H . The results shown are for three different values of α and $\theta = 40^\circ$.

